

The GEOTAIL Magnetic Field Experiment

Susumu KOKUBUN^{1*}, Tatsundo YAMAMOTO², Mario H. ACUÑA³, Kanji HAYASHI¹,
Kazuo SHIOKAWA⁴, and Hideaki KAWANO¹

¹*Department of Earth and Planetary Physics, University of Tokyo, Tokyo 113, Japan*

²*Institute of Space and Astronautical Science, Sagami-hara, Kanagawa 229, Japan*

³*Laboratory for Extraterrestrial Physics, NASA/Goddard Space Flight Center, Greenbelt, MD 20771, U.S.A.*

⁴*Solar Terrestrial Environment Laboratory, Nagoya University, Toyokawa, Aichi 442, Japan*

(Received April 14, 1993; Revised September 1, 1993; Accepted October 25, 1993)

The Geotail spacecraft carries a high-resolution Magnetic Field Experiment to provide magnetic field data in the frequency range below 50 Hz. This experiment includes dual fluxgate magnetometers and a search coil magnetometer. Fluxgate sensors are mounted at distances of 4 m and 6 m from the spacecraft on a deployable mast to reduce spacecraft-generated noises. Both outboard and inboard fluxgate magnetometers have 7 automatically switchable ranges from ± 16 nT to ± 65536 nT (full scale) and resolutions equivalent to a 15-bit A/D conversion in each range. The basic sampling rate for the A/D conversion is 128 Hz for both magnetometers. Sampled signals are averaged to 16 vectors/s for the outboard magnetometer and 4 vectors/s for the inboard magnetometer for telemetry. Time-derivatives of magnetic field in the frequency range of 1–50 Hz (128 vector-samples/s) are acquired by the three-component search coil magnetometer (located on another mast), separated by 4 m from the spacecraft. Fluxgate data are continuously obtained at the same rate for both real-time and recorded modes of operation, while search coil data are only acquired in the real-time telemetry operation.

The instruments were operated after the time of mast deployment on September 4, 1992, and are presently working in all modes as designed. The details of this experiment and initial observations are presented.

1. Introduction

The primary scientific mission of Geotail aims at the understanding of the physics of plasma acceleration processes in the magnetotail and the influx of solar wind energy into the magnetosphere. The magnetic field team will contribute to the mission by measuring magnetic field variations in the frequency range below 50 Hz, using fluxgate and search coil magnetometers. The Geotail mission is divided into two phases (Nishida *et al.*, 1992). During the 2-year initial phase, the orbit apogee is kept on the nightside of the Earth by a series of double-lunar-swing-by maneuvers that result in the spacecraft spending most of its time in the distant magnetotail. The maximum apogee distance achieved is about $220 R_E$ and varies from orbit to orbit.

During its multiple traversals of the distant ($\leq 220 R_E$) magnetotail the ISEE-3 spacecraft played the important role of pathfinder for Geotail and has revealed numerous plasma and field features during both quiet and active periods (e.g. Slavin *et al.*, 1985, 1989; Fairfield *et al.*, 1989). The structure of the magnetotail has been outlined up to about $220 R_E$. Evidence of dynamic behavior has been growing for magnetic merging in the tail, manifested in the form of a large-scale tailward moving magnetic bubble, often referred to as a plasmoid. However, there are still outstanding problems as to the structure and dynamics of the magnetotail, and the plasmoid view is not universally accepted.

* Present address: Solar-Terrestrial Environment Laboratory, Nagoya University, Toyokawa, Aichi 442, Japan.

Observations of field configurations in the region around $100 R_E$, where the neutral line is considered to be formed during quiet conditions, are important to establish the field structure of the magnetotail and its dynamical changes associated with substorms. As for field configurations, it has not yet been known whether or not the magnetotail at $\geq 200 R_E$ is well ordered or filamentary. Some outstanding questions to be examined are: 1) The formation and three dimensional structure of tail plasmoids. 2) Flux rope configurations and their role in the tail dynamics. 3) Large cross-tail magnetic field. 4) The effect of B_y component of the interplanetary magnetic field.

During the second phase of the Geotail mission, the orbit apogee and perigee will be reduced to $30 R_E$ and $8 R_E$, respectively. Important phenomena which can be monitored in the near-tail orbit can be categorized into four classes: Changes due to macroscopic currents, ULF and ELF plasma waves, discontinuities such as the magnetopause and bow shock, and the interplanetary magnetic field. The first class includes magnetopause currents, as well as the ring current, tail current and field aligned-currents coupling the magnetospheric plasma with the ionosphere. The monitoring of magnetic field configuration changes associated with these current systems are very important for understanding the global magnetospheric dynamics of momentum, energy and mass transport during magnetospheric substorms.

During the near-tail operation the spacecraft will skim along the magnetopause boundary on many orbits. Thus, we will have more opportunities to obtain data during multiple crossings of the magnetopause in this experiment than in the previous observations by OGO, IMP and ISEE spacecraft. Magnetic field measurements during such skimming orbits along the magnetopause are useful for study of a transient and localized process such as flux transfer events associated with the solar wind magnetosphere interaction and the study of surface waves on the magnetopause. The second class includes a variety of low-frequency plasma waves whose role in the acceleration process is to be examined in detail. Among them, magnetospheric plasma waves in the ELF range have not yet been surveyed extensively. Thus, we have incorporated the capability to carry out vector measurements of magnetic field variations in the frequency of 1–50 Hz.

During the first phase the spacecraft spends most of the time on the nightside hemisphere. Geotail will also have orbital sections that run nearly parallel to the magnetopause or the bow shock. Interesting data have already been acquired during the magnetopause crossings on October 17 and 18, and November 4 and 5, 1992, as reported in this paper.

Table 1. Magnetometer team.

Principal investigator	Susumu Kokubun	Solar-Terrestrial Environment Laboratory, Nagoya University
Co-investigator	Tatsundo Yamamoto	Institute of Space and Astronautical Science
	Mario H. Acuña	NASA/Goddard Space Flight Center
	Donald H. Fairfield	NASA/Goddard Space Flight Center
	Kanji Hayashi	University of Tokyo
	Takesi Iijima	University of Tokyo
	Kiyofumi Yumoto	Solar-Terrestrial Environment Laboratory, Nagoya University
	Kazuo Shiokawa	Solar-Terrestrial Environment Laboratory, Nagoya University
	Toyohisa Kamei	Kyoto University
	Atsuhiko Nishida	Institute of Space and Astronautical Science
	Yutaka Tonegawa	Tokai University
	Fumio Tohyama	Tokai University
Tohru Sakurai	Tokai University	
Hiroshi Fukunishi	Tohoku University	

The design and development of the magnetometer system was made possible by the cooperation of many people. Data processing and the scientific investigations will rely on the contributions of researchers including the members of the magnetometer team for the scientific investigations listed in Table 1.

2. The Instrument

A fluxgate magnetometer utilizing a ring core geometry was chosen in this experiment because of its robustness and low power. The subsystem for magnetic field measurements (MGF) consists of dual three-axis fluxgate magnetometers and a three-axis search coil magnetometer for measurement of magnetic variations in the frequency range below 50 Hz. A functional block diagram of the system is shown in Fig. 1. The A/D conversion, data processing and automatic range change for the two fluxgate magnetometers are controlled by a microprocessor unit (MPU) in the system. Data from fluxgate magnetometers are sent in the same format for both real time and recorded modes.

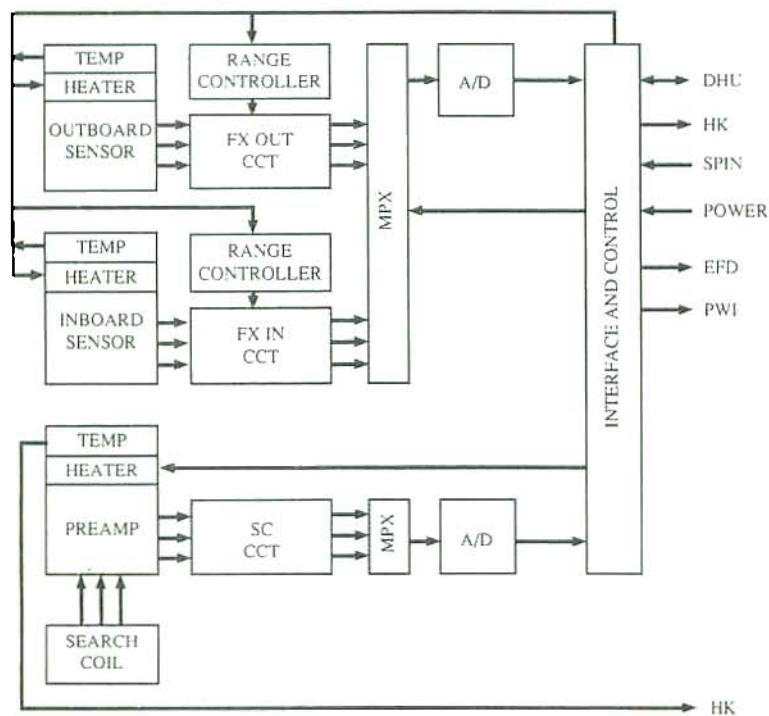


Fig. 1. A functional diagram of the Geotail magnetometer system (MGF).

2.1 Fluxgate magnetometer

The outboard sensor, mounted at the end of a deployable mast (MST-F), is located at a distance of 7.15 m from the spacecraft spin axis. The inboard sensor is mounted on the same mast at a distance of 5.12 m from the spacecraft axis. This configuration allows to monitor spacecraft-generated field changes and also provides redundancy of measurements. The inboard magnetometer (a triad sensor and analog electronics) supplied by the NASA/Goddard Space Flight Center is designed to be similar to those used in successful AMPTE, Voyager and other NASA missions (e.g. Acuña, 1974). The design concept of the outboard magnetometer supplied

by the Institute of Space and Astronautical Science (ISAS) is basically the same as that of the inboard magnetometer.

The fluxgate magnetometers are of standard design and consist of amplifier, filter, phase sensitive detector, integrator and voltage-current converter. Characteristics of the MGF fluxgate magnetometer are summarized in Table 2. Dynamic ranges implemented in previous NASA missions are used in this experiment. Seven dynamic ranges from ± 16 nT to $\pm 65,536$ nT (full scale) are switched automatically whenever the ambient field plus fluctuations exceed a preset level. The automatic operation of range change can be interrupted at any time by ground command.

Table 2. Characteristics of fluxgate magnetometer.

Outboard sensor				
Dimension	140 × 60 × 55 mm			
Weight	340 g + 480 g (cables)			
Heater	2.0 W max			
Inboard sensor				
Dimension	110 × 66 × 69 mm			
Weight	160 g + 360 g (cables)			
Heater	2.0 W max			
Electronics (including search coil electronics)				
Dimension	276 × 282 × 160 mm			
Weight	5.68 kg			
Power	3.51 W (total) 2.52 W (fluxgate magnetometers)			
Dynamic ranges:	± 16 nT; ± 4096 nT;	± 64 nT; $\pm 16,384$ nT;	± 256 nT; $\pm 65,536$ nT	± 1024 nT;
Quantization steps: (15 bit resolution)	0.001 nT; 0.25 nT;	0.004 nT; 1 nT;	0.016 nT; 4 nT	0.0625 nT;
Drive frequency:	14.8 kHz (outboard sensor), 15.0 kHz (inboard sensor),		± 0.5 kHz guard bands ± 0.5 kHz guard bands	
Telemetry rates: (1024 bits/sec)	16 vectors/sec (outboard) 4 vectors/sec (inboard).			

The basic sampling rate with a 16-bit A/D converter (15-bit accuracy) controlled by the MPU, is 128 Hz for both magnetometers. Sampled signals are averaged to 16 vectors/s for the outboard magnetometer and 4 vectors/s for the inboard magnetometer in the normal operation and are sent to the Data Handling Unit (DHU) of the spacecraft and are telemetered to ground. A "swap" mode to change telemetry rates between the outboard and inboard magnetometers is included and can be controlled at any time by ground command. Analog signals from either the outboard or inboard magnetometer are directly fed to the A/D converter for housekeeping in the DHU system to provide backup against malfunctions of the digital control part of the MGF system. Digitized magnetometer signals at the 128 Hz sampling rate are supplied directly to the EFD system to provide ambient field information for the EFD boomerang experiment (Tsuruda *et al.*, 1994).

In order to guarantee compatibility of the two magnetometers, preflight test and intercalibration of the two magnetometers were made for the sensor orientation, offsets, sensitivity factors, and noise levels by using the magnetic facilities both at Kakioka Magnetic Observatory and NASA/Goddard Space Flight Center. Observations indicate that field values obtained by the two sensors are in good agreement with an accuracy better than 0.1 nT.

During the ground test of the spacecraft, significant efforts were made to reduce spacecraft-generated DC/AC fields in cooperation with many people including members of the Plasma Wave Instrument (PWI) team and other scientific and engineering teams. As a result, the wiring inside the spacecraft was redesigned and refabricated, and the electromagnetic environment for scientific measurements was greatly improved. We confirmed during the preflight tests that the bias field from the spacecraft would be smaller than 1 nT at the location of the outboard sensor.

2.2 Search coil magnetometer

The search coil magnetometer system consists of three sensors, preamplifier, main-amplifier, filters, multiplexers and a 12-bit A/D converter. The instrument summary is given in Table 3. The design of sensor and pre-amplifier is basically the same as that of EXOS-D satellite (Fukunishi *et al.*, 1990). Three search coils are orthogonally mounted at a distance of 4.10 m on another 6 m mast (MST-S) together with search coils for VLF wave measurements at the tip of the mast. A preamplifier with an open loop gain of 60 dB is mounted close to the sensors to reduce the interference from spacecraft-generated noise. The output of the pre-amplifier is proportional to the time derivative of field component in the frequency range of 1–50 Hz as is seen in Fig. 7 of Fukunishi *et al.* (1990). The three gain ranges of the main amplifier (*L*; 20 dB, *M*; 40 dB, *H*; 60 dB) can be changed by ground command. Medium gain has been used in routine operations since September 1992. Digitization of signals is made at the rate of 128 Hz to transmit wave form signals below 50 Hz. This wave form measurement in the ELF frequency range is only operated in the real-time mode of which the telemetry reception is done at Usuda Deep Space Center of ISAS. Signals detected by the search coil sensors of the MGF system are also used in the PWI system (Matsumoto *et al.*, 1994).

Table 3. Characteristics of search coil sensor and preamplifier.

Sensor	Three coils with 10^5 turns of copper wire ($\phi = 0.05$ mm ϕ)
Core material and Dimension	4–79 Mo/Ni permalloy
Sensor dimension	$3 \times 3 \times 300$ mm (0.05 mm \times 60 layers)
	$14 \times 14 \times 305$ mm for one component (including an aluminum static shield case)
Pre-amplifier	
Gain	60.3 dB
Volume	$100 \times 80 \times 30$ (mm) ³
Power	0.1 W
Heater	2.0 W max
Weight	
Sensors	500 g
Pre-amplifier	380 g
Cables	340 g
Frequency range	0.5 Hz–1 kHz

3. Data Processing

Absolute zero levels may be deduced by reversal of the two components transverse to the spin axis. However, it is not easy to determine field offset of the component parallel to the spin axis. Thus, the techniques for determination of zero levels by using inflight data have been discussed extensively (e.g. Hedgecock, 1975). We have tried to use data obtained during the mast

deployment. But unfortunately, the spacecraft entered the magnetosheath where magnetic fields were very turbulent during the mast extension. We have difficulties in determining the field offset with an accuracy better than 0.1 nT at the sensor location by using the data obtained during the mast extension. At present, we can state that the bias field is smaller than 0.5 nT at the outboard sensor location.

A long-term trend of differences in observed Z magnetic fields between the inboard and outboard sensors is being studied to verify the validity of the nominal Z offsets. We have also compared the results from the EFD-Boomerang experiments which provide us with the electron gyroperiod with high accuracy. These results will be reflected to update the values of the zero levels and their accuracy.

As part of the International Solar Terrestrial Physics (ISTP) program, the Central Data Handling Facility (CDHF)/NASA will process the level-zero spacecraft data into overview or summary data, called "key parameters", for the scientific community. We will provide 64 sec.-averages of magnetic field as key parameters.

4. Initial Observations

Deployment of the masts for the MGF and PWI systems was done on September 4, 1992, but the MST-S mast for the search coil magnetometers was only partially deployed. Deployment of MST-S was completed on September 16. Routine observations began after the completion of mast deployment. During the first five months of observation, we have obtained very interesting data near the dayside magnetopause as well as in the distant magnetotail. We observed multiple crossings of the magnetopause around the dawn flank of the magnetosphere during two successive inbound orbits on October 17 and November 4, 1992. Examples of magnetic field variations are discussed in the following paragraphs.

Figure 2 shows an example of MGF data, including search coil (SC) data, observed in the distant tail. The spacecraft was in the northern tail lobe ($X_{GSM} = -78$, $Y_{GSM} = 0$; $Z_{GSM} = 5 R_E$) on October 24, 1992. Magnetic field data are plotted in satellite coordinates in which the X axis is directed to the sun and the Z axis is parallel to the spin axis. The fourth panel (SC Z) indicates dynamic spectra as measured by the search coil whose axis is parallel to the spin axis. Variations of satellite potential measured with the EFD single probe (Tsuruda *et al.*, 1994) are shown in the bottom panel. Single probe data provide a measure of plasma density. An increase in negative potential means a decrease in plasma density (Tsuruda *et al.*, 1994).

A series of peculiar magnetic perturbations were registered for about one hour period starting at 1525 UT. A decrease in B_x with fluctuations in all components after 1900 indicates that the spacecraft entered into the plasma sheet. Burst-like ELF emissions were observed in the frequency range of 10–50 Hz in association with the spacecraft entry into the plasmashet. Similar ELF bursts are often observed around the plasma sheet boundary layer. An expanded plot of the two hour interval from 1500 to 1700 UT is shown in Fig. 3. A combination of a bipolar perturbation in the B_y component and a W-shaped perturbation in the B_z component was observed around 1532 UT. This type of perturbation was also observed with ISEE 3 and was associated with a magnetic flux rope structure (Sibeck *et al.*, 1984). Single probe data suggest a small enhancement in the plasma density in the flux rope, consistent with the ISEE 3 observations.

Particular magnetic field variations successively appear in a similar form at 1547, 1601, 1622, and 1655 UT. At these times the B_z component shows a bipolar perturbation and the field strength a unipolar enhancement. This type of perturbation, called "Travelling Compression Region (TCR)", was first reported by Slavin *et al.* (1984). The present observation indicates that no clear change in the plasma density and in the ELF wave activity are associated with TCR's. According to ISEE 3 observations, flux rope structures are associated with ground magnetic activity. The occurrence of substorm-generated plasmoids traveling down the magnetotail is

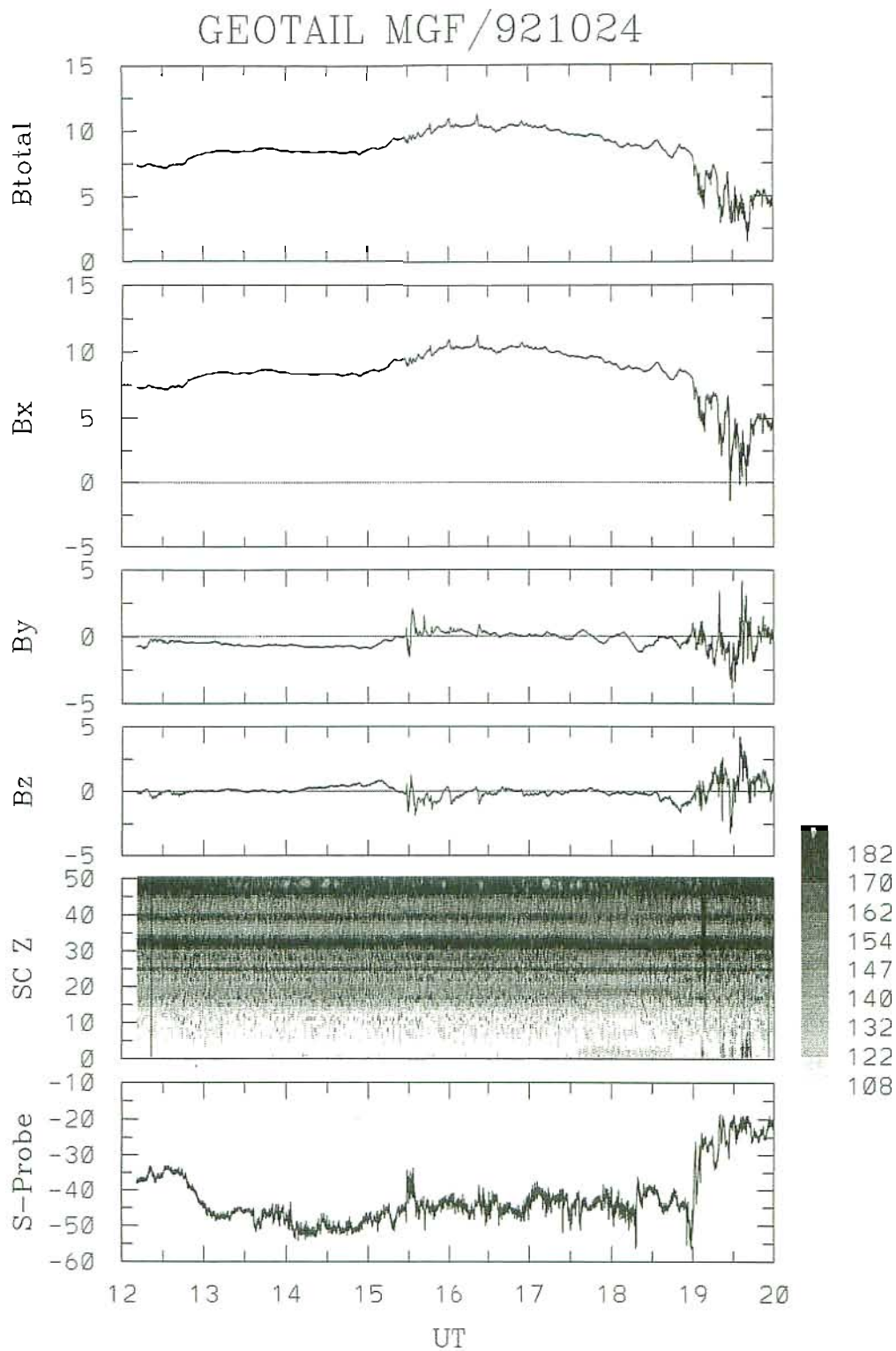


Fig. 2. An example of magnetometer data plot along with the EFD single probe data. Geotail was in the northern tail lobe ($X_{GMS} = -78$, $Y_{GMS} = 0$, $Z_{GMS} = 5 R_E$) on October 24, 1992. Upper three panels show fluxgate magnetometer data (nT) in satellite coordinates in which the X axis directs toward the sun and the Z axis is parallel to the spin axis. The fourth panel indicates dynamic spectra of signals from the search coil sensor along the spin axis (8 sec. averaged spectra). In the bottom panel is shown variations of satellite potential measured with the single probe in the EFD experiment (Tsuruda *et al.*, 1994).

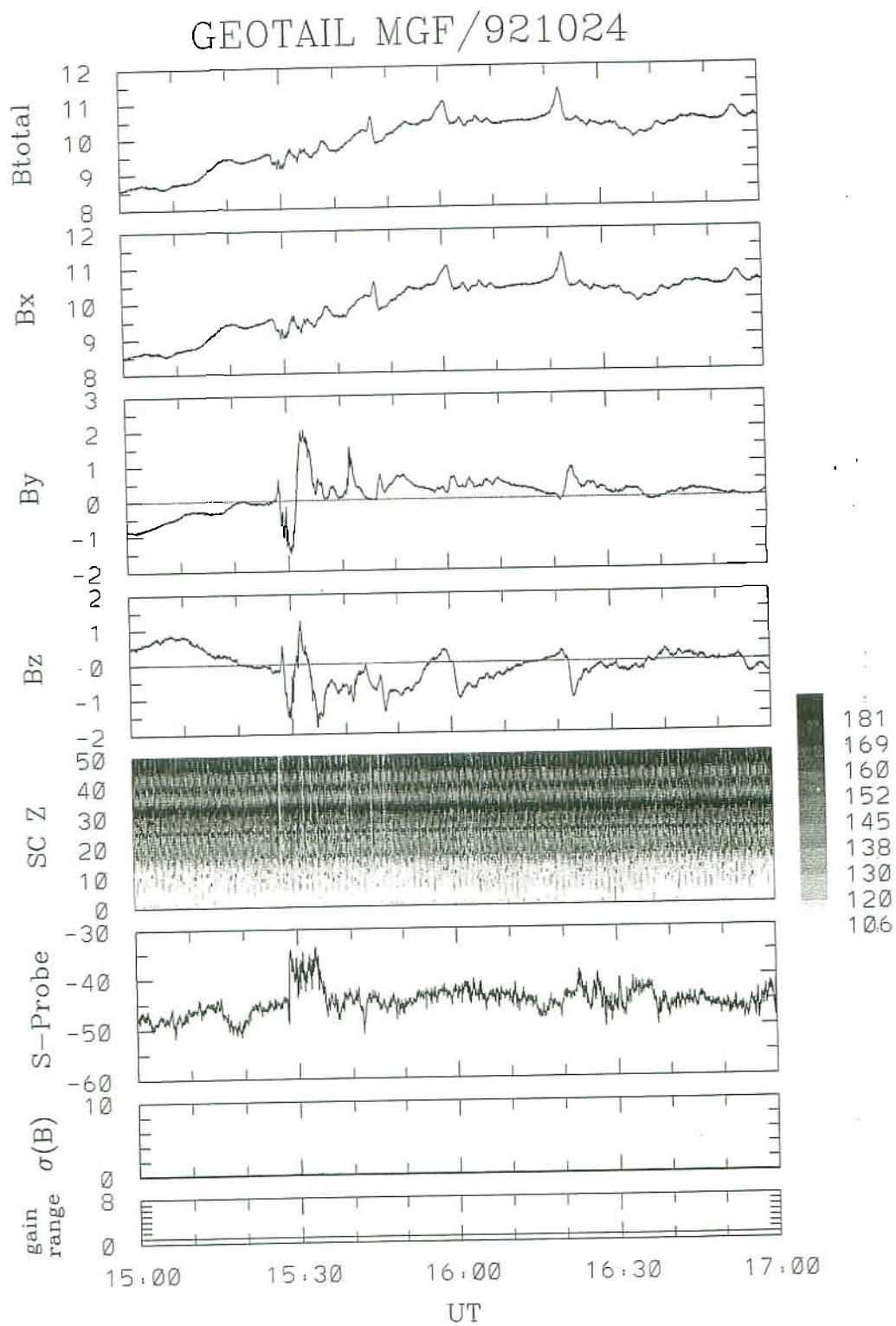


Fig. 3. An expanded plot of magnetic field data obtained in the distant tail (in GSE coordinates).

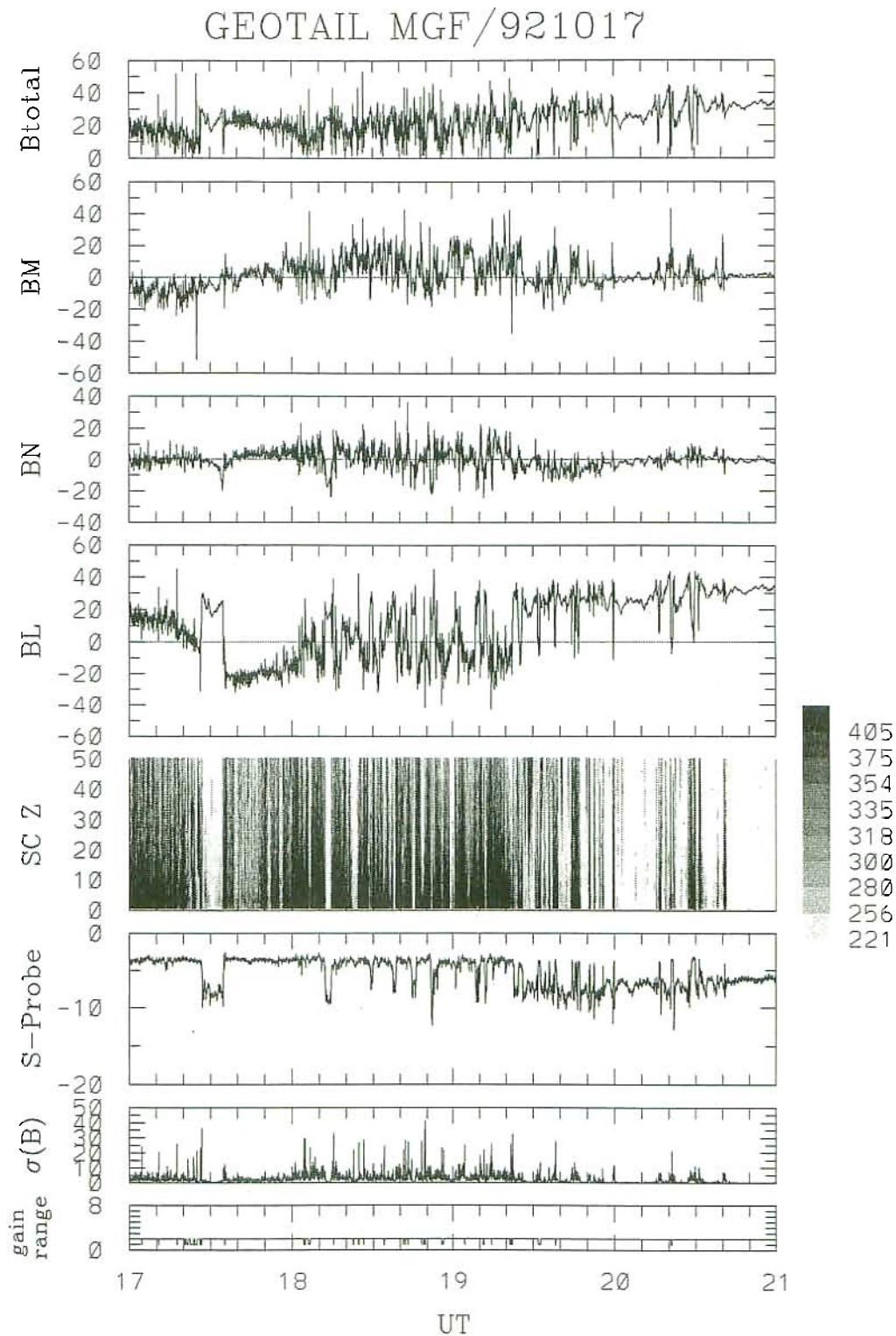
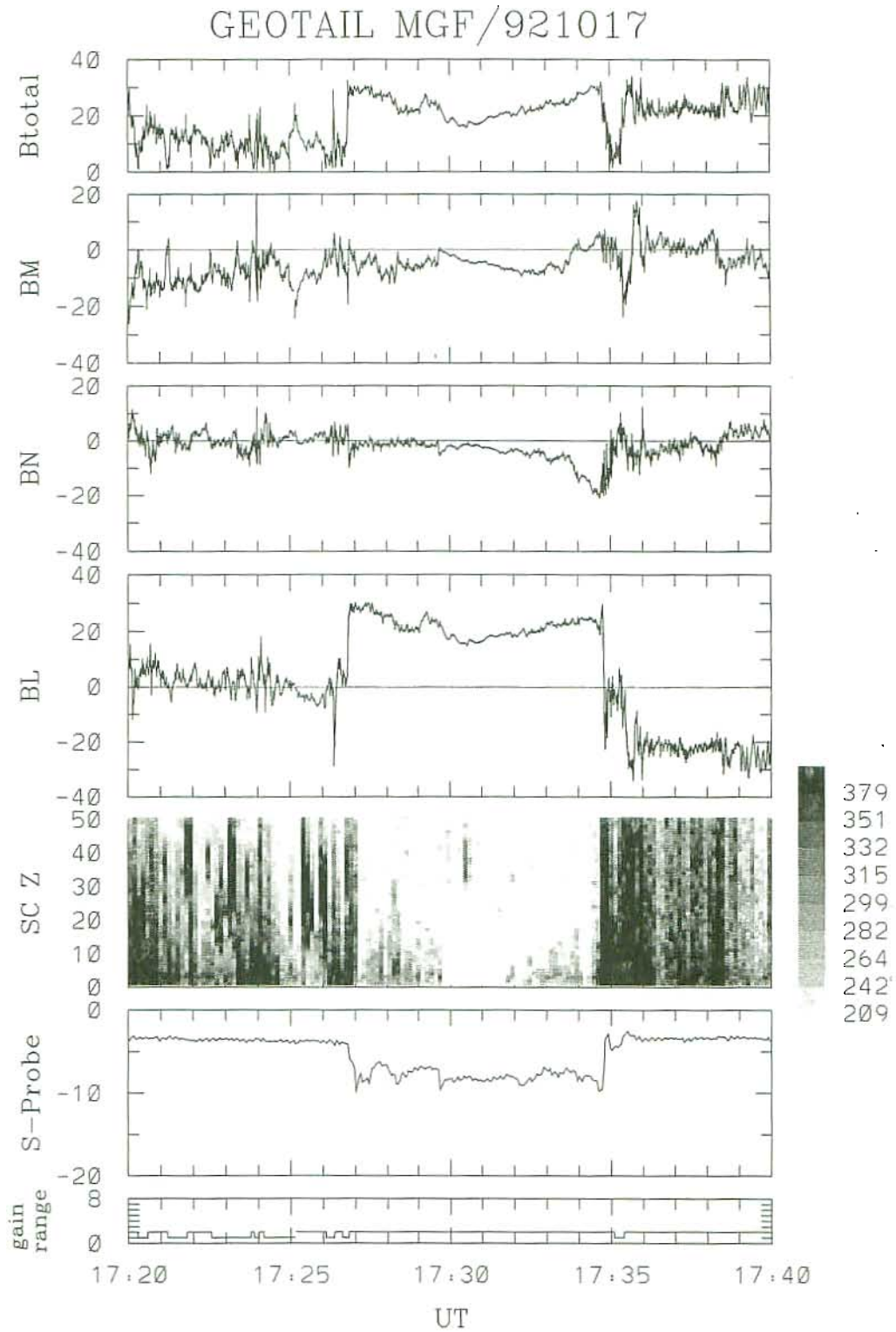
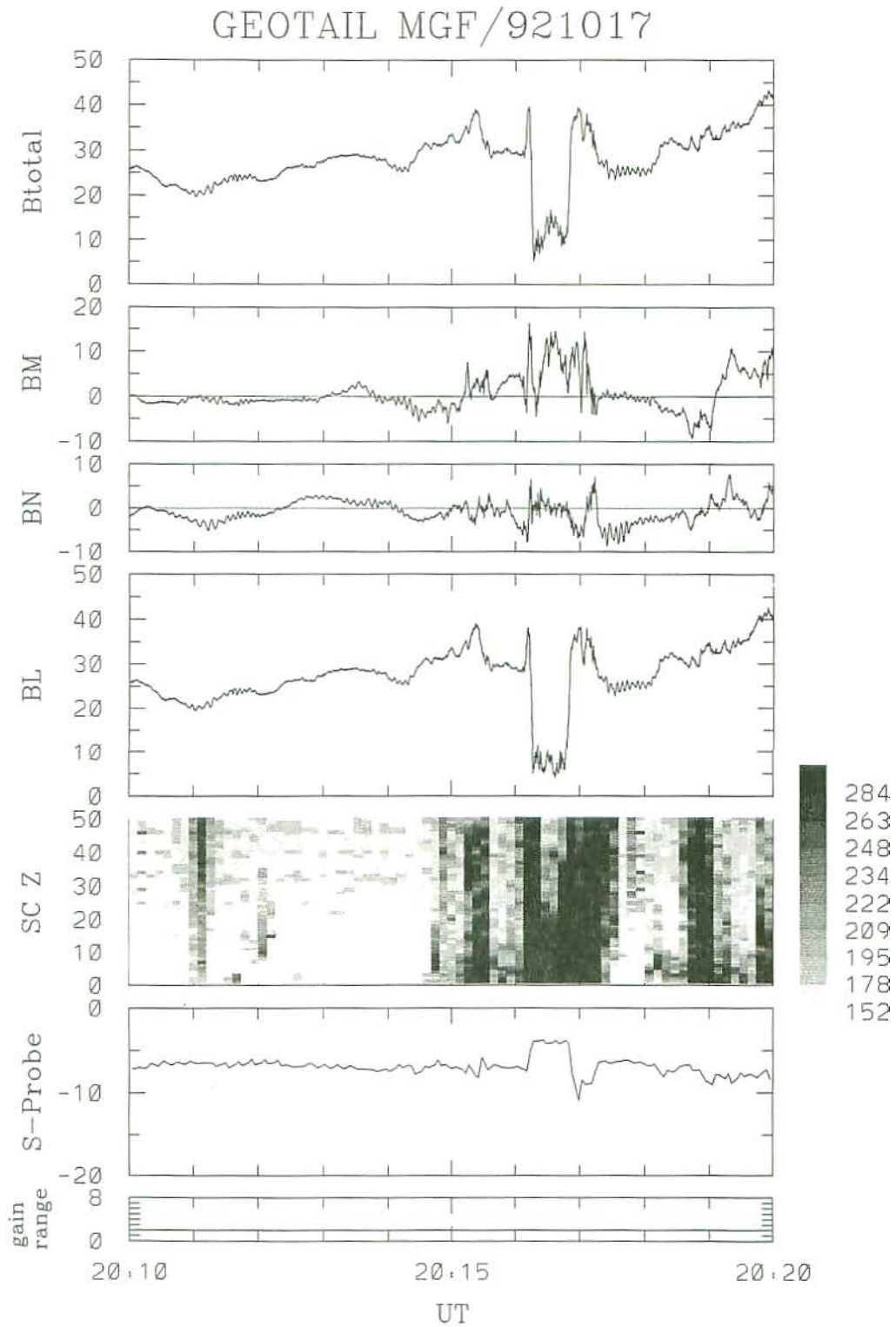


Fig. 4. A series of magnetopause crossings as observed on the morning flank on October 17, 1992. Four hour data are plotted in boundary normal coordinates along with ELF spectra and satellite potential. The spacecraft position for 1700–2100 was on the morning side (1.8, -15.1, 4.3, -5.3, -10.6, 1.0, in GSM). Large variations in the B_L component indicate that multiple crossings occurred during southward magnetosheath fields.



(a)

Fig. 5. Examples of high resolution fluxgate measurements (16 samples per second) across the magnetopause on October 17, 1992.



(b)

Fig. 5. (continued).

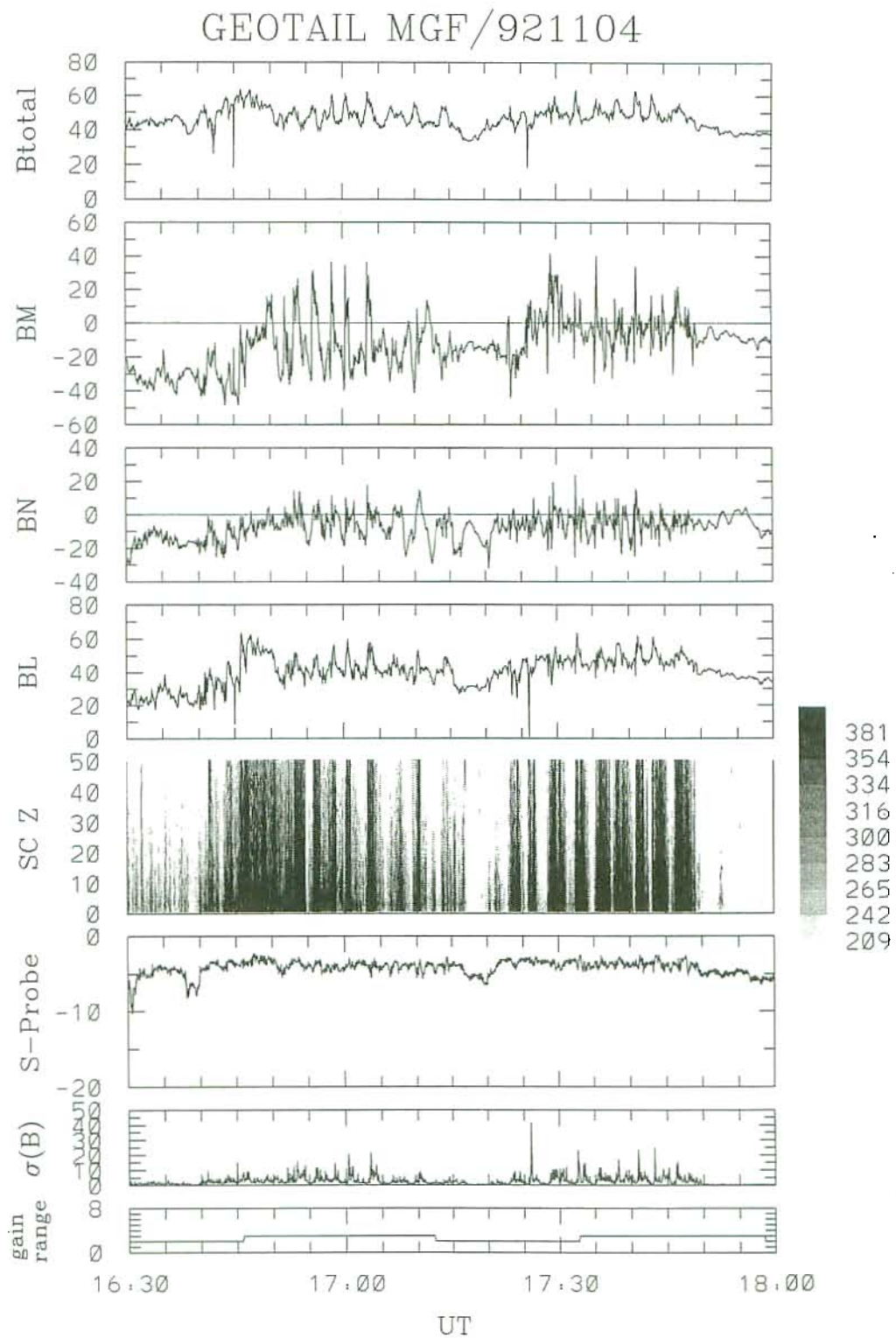


Fig. 6. Quasi-periodic oscillations of magnetic field observed near the dawn flank of the magnetosphere on November 4, 1992. The position of Geotail at 1700 UT was $(-1.4, -14.3, -1.3)$ [R_E] in GSE coordinates. Magnetic field oscillations are largest in the B_M component. Appearances of repetitive ELF bursts correspond to peaks in the B_M component. In contrast to the previous example satellite potential did not show significant oscillation.

considered to produce the TCR events in the lobe during their passages. Ground magnetic activity, however, was rather quiet during the period when flux rope structures and traveling compression regions were observed on October 24.

Interesting data on multiple magnetopause crossings were obtained during the four-hour period (1700–2100 UT) on October 17 in association with southward sheath magnetic fields. Figure 4 indicates magnetic variations in boundary normal (LMN) coordinates (Russell and Elphic, 1978). In this system the N -direction is normal to the magnetopause pointing outward, the L -direction is a projection of the GSM Z axis to the plane tangent to the magnetopause, and the M -direction completes the (L, M, N) triad. We use the recent model of the magnetopause shape derived by Sibeck *et al.* (1991). As is seen from the figure, magnetic field fluctuations are too complex to identify magnetopause crossings from magnetic field data only. We can identify the entry of the spacecraft into the magnetosphere from an increase in negative satellite potential and a fadeout of ELF bursts. The first crossing around 1727 UT occurred during a southward excursion of the sheath magnetic field. The spacecraft was mostly in the magnetosheath and occasionally entered into the magnetosphere before 1922 UT. Transient exits of Geotail from the magnetosphere were observed from 1922 to 2040 UT. Although more than 20 pairs of magnetopause crossings were identified in this inbound orbit, crossings were found to occur sporadically without periodicity.

Figure 5a shows the full resolution of the fluxgate magnetometer measurements for the first pair of traverse. The Geotail was in the magnetosphere from 17:26:50 to 17:34:40 UT. A sharp contrast of ELF wave spectra is very evident between the magnetosphere and magnetosheath. It is also noted that boundary traverses were observed during short periods of 10–20 seconds. A transient exit of the spacecraft from the magnetosphere during northward sheath fields is illustrated in Fig. 5b. Strong ELF bursts extending above 50 Hz were observed near the magnetopause in both cases. Fig. 5b also shows that Pc 1 waves with periods of several seconds appeared close to the magnetopause.

During the next magnetopause-skimming orbit on the morningside on November 4, 1992 we observed quasi-periodic oscillations of magnetic field with a period of approximately two minutes during the interval from 1645 to 1750 UT. Figure 6 displays a MGF data plot along with single probe data during the one and a half hour interval starting at 1630 UT. Quasi-periodic oscillations in B_M are clearly seen in the intervals of 1651–1705 UT and 1720–1750 UT. It is interesting to note here that the occurrence of repetitive ELF bursts, showing magnetosheath signatures, corresponds to maxima in the magnetic field magnitude. We cannot see clear quasi-periodic variations in the single probe data. This suggests that no significant change in plasma density is associated with these oscillations. Thus, the spacecraft is entering into the low latitude boundary layer and going out to the magnetosheath alternately.

The oscillating component of magnetic field is largest along the B_M direction. Peaks in the B_M component are associated with the occurrence of ELF bursts. We have applied a minimum variance analysis (Sonnerup and Cahill, 1967) to this event. Figure 7 shows magnetic variations in minimum variance coordinates. A comparison between Figs. 6 and 7 shows that field variations in the B_M component and in the B1 component are essentially similar to each other. Thus, the oscillating component of the magnetic field is mostly tangential to the expected magnetopause boundary.

Both series of magnetopause crossings were observed on the dawn flank of the magnetosphere, but the characteristics of magnetic field changes were essentially different, presumably due to the difference in the direction of the interplanetary magnetic field. The former instance was associated with southward magnetosheath fields. On the other hand, strong northward magnetic fields were observed in the magnetosheath in the latter case. Furthermore, field magnitudes outside the magnetopause were larger than those in the magnetosphere. More detailed analysis is needed to clarify these characteristic differences in the two examples of magnetopause crossing events.

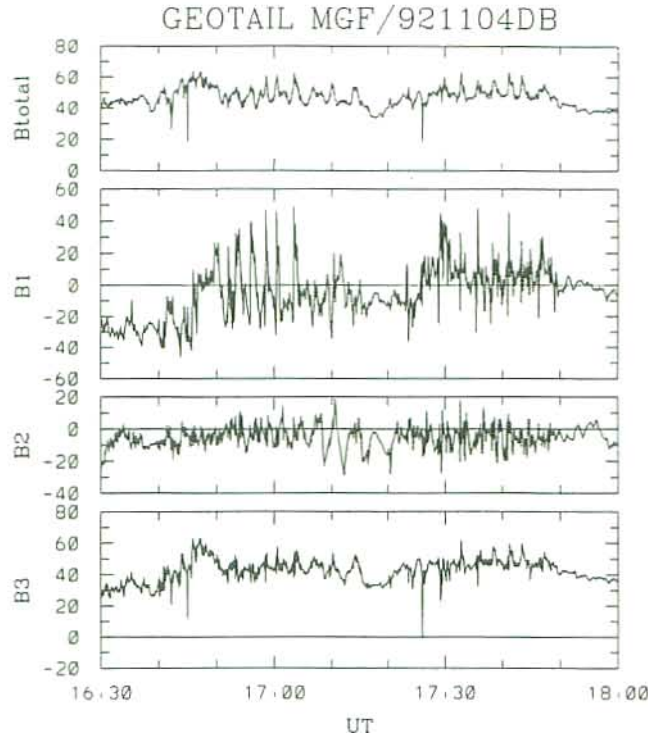


Fig. 7. The minimum variance analysis technique is applied to the magnetic field data in the period from 1651 UT to 1705 UT, during which period the magnetic field oscillation is very clear. The magnetic field components, B1, B2, and B3, correspond to the directions of maximum, intermediate, and minimum variances, and standard deviations are 18.5, 5.7, and 4.1 [nT], respectively. Polar angles of the unit vectors, E1, E2, and E3, are (94.1, -138.9), (89.7, -48.9), and (4.1, 36.7) [degree] in the GSE coordinates.

5. Concluding Remarks

The MGF system consisting of fluxgate and search coil magnetometers is presently working well in all modes as designed. The quality of data obtained is found to be excellent without significant contamination of spacecraft-generated signals. Temperatures of the sensor assemblies were increasing slightly probably due to the increase in solar radiation during the northern winter, but no problems have occurred with this temperature increase. Drift of zero levels of the outboard fluxgate magnetometer is estimated to be about 0.05 nT/°C. Further improvement in determination of zero levels will be done in the near future.

We are grateful to the Institute of Space and Astronautical Science and the National Aeronautics and Space Administration for making Geotail a reality. The final design, packaging and fabrication of the MGF system were skillfully directed by M. Abe, S. Shinoda, and T. Omoto of Meisei Electric Company. NCAR Graphics packages are used to make all figures but Fig. 1.

REFERENCES

- Acuña, M. H., Fluxgate magnetometers for outer planets exploration, *IEEE Trans. Magn.*, **MAG-10**, 519-523, 1974.
- Fairfield, D. H., D. N. Baker, J. D. Craven, R. C. Elphic, J. F. Fennel, L. A. Frank, I. G. Richardson, H. J. Singer, J. A. Slavin, B. T. Tsurutani, and R. D. Zwickl, Substorms, plasmoids flux rope, and magnetotail flux loss on March 25 1983: CDAW 8, *J. Geophys. Res.*, **94**, 15135-15152, 1989.

- Fukunishi, H., R. Fujii, S. Kokubun, K. Hayashi, T. Tohyama, Y. Tonegawa, S. Okano, M. Sugiura, K. Yumoto, I. Aoyama, T. Sakurai, T. Saito, T. Iijima, A. Nishida, and M. Natori, Magnetic field observations on the AKEBONO (EXOS-D) satellite, *J. Geomag. Geoelectr.*, **42**, 385–409, 1990.
- Hedgecock, P. C., A correlation technique for magnetometer zero level determination, *Space Sci. Instr.*, **1**, 83–90, 1975.
- Matsumoto, H., I. Nagano, R. R. Anderson, H. Kojima, K. Hashimoto, M. Tsutsui, T. Okada, I. Kimura, Y. Omura, and M. Okada, Plasma wave observations with the GEOTAIL spacecraft, *J. Geomag. Geoelectr.*, this issue, 59–95, 1994.
- Nishida, H., K. Uesugi, I. Nakatani, T. Mukai, D. H. Fairfield, and M. H. Acuña, Geotail mission to explore Earth's magnetotail, *EOS, Trans. AGU*, **73**, No. 40, Oct. 6, 1992.
- Russell, C. T. and R. C. Elphic, Initial ISEE magnetometer results: Magnetopause observations, *Space Sci. Rev.*, **22**, 681–715, 1978.
- Sibeck, D. G., G. L. Siscoe, J. A. Slavin, E. J. Smith, S. J. Bame, and F. L. Scarf, Magnetic flux ropes, *Geophys. Res. Lett.*, **11**, 1090–1093, 1984.
- Sibeck, D. G., R. E. Lopez, and E. C. Roelof, Solar wind control of the magnetopause shape, location, and motion, *J. Geophys. Res.*, **96**, 5489–5495, 1991.
- Slavin, J. A., E. J. Smith, B. T. Tsurutani, D. G. Sibeck, H. J. Singer, D. N. Baker, J. T. Gosling, E. W. Hones, and F. L. Scarf, Substorm associated traveling compression regions in the distant tail: ISEE-3 geotail observations, *Geophys. Res. Lett.*, **11**, 675–678, 1984.
- Slavin, J. A., E. J. Smith, D. G. Sibeck, D. N. Baker, R. D. Zwickl, and S.-I. Akasofu, An ISEE 3 study of average and substorm conditions in the distant magnetotail, *J. Geophys. Res.*, **90**, 10874–10895, 1985.
- Slavin, J. A., D. N. Baker, J. D. Craven, R. C. Elphic, D. H. Fairfield, L. A. Frank, A. B. Galvin, W. J. Hughes, R. H. Manka, D. G. Mitchell, I. G. Richardson, T. R. Sanderson, D. J. Sibeck, E. J. Smith, and R. D. Zwickl, CDAW 8 observations of plasmoid signatures in the geomagnetic tail: An assessment, *J. Geophys. Res.*, **94**, 15153–15175, 1989.
- Sonnerup, B. U. O. and L. J. Cahill, Jr., Magnetopause structure and altitude from Explorer-12 observations, *J. Geophys. Res.*, **72**, 171–183, 1967.
- Tsuruda, K., H. Hayakawa, M. Nakamura, M. Nakamura, T. Okada, A. Matsuoka, F. S. Mozer, and R. Schmidt, Electric field measurement on the Geotail satellite, *J. Geomag. Geoelectr.*, 1994 (submitted).